13th Spring School on Transition and Turbulence
September 19th-23rd, 2022, Blumenau, SC, Brazil

EPTT-2022-XXXX
REVISED AND EXTENDED RESULTS ON A LAMINAR PERTURBED FLOW TOWARDS CALIBRATION OF A KINETIC ENERGY – HELICITY TURBULENCE MODEL

José Ricardo Figueiredo
FEQ, UNICAMP - Cidade Universitária Zeferino Vaz - Barão Geraldo, Campinas - SP, 13083-970
jrfigue@fem.unicamp.br

Abstract. *Fluctuating velocities and pressures at selected points of an oscillated laminar flow are recoded and processed to provide the statistical correlations of the transport equations for kinetic energy, helicity and enstrophy. The primitive variables solver uses UNIFAES discretization for the advective and viscous terms. Such scheme is generalized by making explicit the space derivatives employed in the solver, allowing its use in the calculation of the various correlations, in parallel with second order and forth order central differencing schemes.*

Keywords: *Generalized UNIFAES, kinetic energy, helicity, enstrophy.*

1. INTRODUCTION

The construction of a turbulence model based on fluctuating kinetic energy and helicity was proposed by Figueiredo (2018b). Helicity is the scalar product of velocity and vorticity. Such concept was formulated about 1960, with applications in meteorology and magneto-hydrodynamics (Moffatt and Tsinober, 1992). Fluctuations in helicity have been associated to turbulence cascade and vortex stretching in physics literature (Holm, 2007; Dallas and Tobias, 2016; Yan et al., 2020). However, helicity is absent from the literature on statistical models of turbulence for engineering.

The primitive variables incompressible Navier-Stokes solver applies to three-dimensional flows, using UNIFAES scheme for the advective and viscous transport terms, semi-staggered mesh, Poisson equation for pressure with momentum interpolation, and forth order Runge-Kutta time-wise integration. Instantaneous velocity and pressure around selected nodes are recorded to be processed in the program for the statistical correlations of the transport equations for kinetic energy, helicity and enstrophy. Testing of the statistics program used an oscillated laminar flow, which can be analyzed with modest refinement levels allowed by a personal computer.

Initial results concerning this proposal (Figueiredo, 2020) are revised, an important error on the helicity transport equation is corrected, and, particularly, coherence between the numerical methods of the Navier-Stokes solver and those of the statistical correlations is improved through a generalization of UNIFAES which turned explicit its first and second derivatives, so that the correlations can be calculated with the same interpolating curve of the solver.

2. GENERALIZED UNIFAES SCHEME

UNIFAES computes the combined advective and diffusive terms without requiring its first and second derivatives, which are made explicit here. This work is restricted to regularly spaced Cartesian meshes, although UNIFAES admits irregularly spaced meshes without loss of second order convergence, with adequate refinement route (Llagostera and Figueiredo, 2000a, 2000b).

UNIFAES applies to the divergence form advective term and diffusive term of the transport equation of a transported variable Φ on a velocity field $\mathcal{U}_i$:

$$\frac{\partial \Phi}{\partial t} + \frac{\partial \mathcal{U}_i \Phi}{\partial x_i} - \nu \frac{\partial^2 \Phi}{\partial x_i \partial x_i} = S \tag{1}$$

Here, ν is the diffusivity of the transported variable and S is a possible source term. Summation over the three coordinate directions is assumed for each repeated index in a term.

The Finite Volume analogue of the net advective and diffusive flux $\partial J_1/\partial x_1$ is:

$$\frac{\partial J_1}{\partial x_1} \cong \frac{J_e - J_w}{\Delta x_1} = \frac{1}{\Delta x_1 \Delta x_2 \Delta x_3} \int_{x3_d}^{x3_u} \int_{x2_s}^{x2_n} \int_{x1_w}^{x1_e} \left(\frac{\partial \mathcal{U}\Phi}{\partial x_1} - \upsilon \frac{\partial^2 \Phi}{\partial {x_1}^2} \right) dx_1\, dx_2 dx_3 \cong \frac{1}{\Delta x_1} \left[\mathcal{U}_e \Phi_\mathrm{e} - \upsilon \frac{\partial \Phi}{\partial x_{1_e}} - \mathcal{U}_w \Phi_\mathrm{w} + \upsilon \frac{\partial \Phi}{\partial x_{1_w}} \right] \tag{2}$$

Division by cell volume is used above to restore the physical dimension of the original equation, as convenient for expressing derivatives. Exponential-type schemes employ interpolating curves obtained as exact solutions of the one-dimensional linear equation:

$$\mathcal{U}\frac{d\Phi}{dx} - \nu\frac{d^2\Phi}{dx^2} = K \tag{3}$$

Equation (3) approximates transport equation (1) considering the velocity component $\mathcal{U}$ in direction x to be locally constant, as well as term K, which represents all other terms of the equation (1), namely cross flow transport, source and transient terms. The resulting interpolation curve is:

$$\Phi = C_1 + C_2 exp\left(\frac{\mathcal{U}.x}{\nu}\right) + \frac{K}{\mathcal{U}}x \tag{4}$$

The Finite Volume Exponential-type schemes employ the interpolating curve (4) to determine the flux through cell face *e*, for instance, using reference properties at such face. Curve (4) is fit to nodes P e E, with origin at node P, yielding:

$$C_2 = \frac{\Phi_\mathrm{E} - \Phi_\mathrm{P} - \frac{K_e}{\mathcal{U}_e}\Delta x}{exp\left(\frac{\mathcal{U}_\mathrm{e}\Delta x}{\nu}\right) - 1} \tag{5}$$

$$C_1 = \Phi_\mathrm{P} - C_2 \tag{6}$$

Deriving $\Phi(x)$ from Equation (3) :

$$\frac{d\Phi}{dx} = C_2\frac{\mathcal{U}}{\nu}exp\left(\frac{\mathcal{U}.x}{\nu}\right) + \frac{K}{\mathcal{U}} \tag{7}$$

Profile (4) and its derivative (7) are then employed to compute the advective – diffusive flux. At cell face *e* it results, in terms of the cell face Peclet number $p_e = \mathcal{U}_e\Delta x_1/\nu$:

$$J_e = \mathcal{U}_e\Phi_\mathrm{e} - \nu\frac{\partial\Phi}{\partial x}_e = \mathcal{U}_e C_1 + K\left(x_e - \frac{\nu}{\mathcal{U}_e}\right) = (\Phi_P - \Phi_E)\nu\frac{\pi(p_e)}{\Delta x_1} + K_e\left[\frac{\pi(p_{e/w}) - 1}{p_{e/w}} + \frac{1}{2}\right] + \mathcal{U}_e\Phi_P \tag{8}$$

Proceeding analogously for the west side and substituting into (2), the combined advective-diffusive net flux through east and west faces is:

$$\frac{J_e - J_w}{\Delta x_1} \cong \frac{1}{\Delta x_1}\left[\nu\frac{\pi(p_e)}{\Delta x_1}(\Phi_P - \Phi_E) + \nu\frac{\pi(p_w)}{\Delta x_1}(\Phi_P - \Phi_W) + \Psi + (\mathcal{U}_e - \mathcal{U}_w)\Phi_P\right] \tag{9}$$

$$\pi(p_{e/w}) = \frac{p_{e/w}}{exp(p_{e/w}) - 1} \tag{10}$$

$$\Psi = K_e\chi(p_e) - K_w\chi(p_w) \tag{11}$$

$$\chi(p_{e/w}) = \frac{\pi(p_{e/w}) - 1}{p_{e/w}} + \frac{1}{2} \tag{12}$$

Term $(\mathcal{U}_e - \mathcal{U}_w)\Phi_P/\Delta x_1$ and its analogues for other directions vanish due to continuity.

Terms K are determined in UNIFAES by Allen and Southwell´s (1955) Exponential scheme. Unknowns C_1, C_2 and $K_P/\mathcal{U}_P$ of curve (4) are fit to the nodes W, P and E, using properties of node P, forming a system that can be solved for K_P in terms of cell Peclet number $p_P = \mathcal{U}_P\Delta x/\upsilon$:

$$K_P = (\Phi_P - \Phi_E)\frac{\pi(p_P)}{\Delta x^2} + (\Phi_P - \Phi_W)\frac{\pi(-p_P)}{\Delta x^2} \tag{13}$$

$$\pi(p_P) = \frac{p_P}{exp(p_P) - 1} \tag{14}$$

UNIFAES determines K_e by interpolating between the estimates of K_P, Eq. (13), and analogous for K_E. If node E is located at a wall, K_e is obtained by extrapolation from K_P and K_W.

The Finite Volume analogues of the first and second derivatives in direction x_1 are obtained by integration on the cell volume using the divergence theorem:

$$\frac{1}{\Delta x_1}\int_{x1_w}^{x1_e}\frac{\partial\Phi}{\partial x_1}dx_1 = \frac{\Phi_e-\Phi_W}{\Delta x_1} \tag{15}$$

$$\frac{1}{\Delta x_1}\int_{x1_w}^{x1_e}\frac{\partial^2\Phi}{\partial x_1{}^2}dx_1 = \left(\frac{\partial\Phi}{\partial x_{1e}}-\frac{\partial\Phi}{\partial x_{1w}}\right)\frac{1}{\Delta x_1} \tag{16}$$

From the interpolating curve (4), using constants (5) and (6), one obtains for the cell face *e*:

$$\Phi_e = \Phi_P + \frac{\Phi_E-\Phi_P-\frac{K_e}{u_e}\Delta x}{exp(p_e)-1}\left[exp(p_e/2)-1\right] + \frac{K_e}{u_e}\frac{\Delta x}{2} \tag{17}$$

Proceeding analogously for the west side, one gets UNIFAES first derivative:

$$\frac{\Phi_e-\Phi_w}{\Delta x_1} = \frac{(\Phi_E-\Phi_P)\Theta(p_e)-(\Phi_W-\Phi_P)\Theta(-p_w)}{\Delta x_1} + \frac{K_e}{\upsilon}\Delta x.\Omega(p_e) - \frac{K_w}{\upsilon}\Delta x.\Omega(-p_w) \tag{18}$$

$$\Theta(p) = \frac{exp(p/2)-1}{exp(p)-1} = \frac{1}{exp(p/2)+1} \tag{19}$$

$$\Omega(p) = \frac{\frac{1}{2}-\Theta(p)}{p} = \frac{exp(p/2)-1}{2p(exp(p/2)+1)} = \frac{\Theta(p)}{4\pi(p/2)} \tag{20}$$

Using Eq. (7) with constants (5) and (6), one obtains for the cell face *e*:

$$\frac{\partial\Phi}{\partial x}_e = \frac{\Phi_E-\Phi_P+\frac{K_e}{u_e}\Delta x}{exp(p_e)-1}.\frac{p_e}{\Delta x}.exp\left(\frac{p_e}{2}\right) + \frac{K_e}{u_e} \tag{21}$$

By proceeding analogously for face *w* one obtains UNIFAES second derivative:

$$\left(\frac{\partial\Phi}{\partial x}_e - \frac{\partial\Phi}{\partial x}_w\right)\frac{1}{\Delta x} = \frac{\Phi_E-\Phi_P}{\Delta x^2}\lambda(p_e) + \frac{\Phi_W-\Phi_P}{\Delta x^2}\lambda(-p_w) + \frac{K_e}{\upsilon}.\Upsilon(p_e) + \frac{K_w}{\upsilon}.\Upsilon(-p_w) \tag{22}$$

$$\lambda(p) = \frac{p.exp\left(\frac{p}{2}\right)}{exp(p)-1} = \pi(p)exp\left(\frac{p}{2}\right) \tag{23}$$

$$\Upsilon(p) = \frac{1-\pi(p)exp\left(\frac{p}{2}\right)}{p} \tag{24}$$

Paradoxically, the generalized UNIFAES derivatives are non-linear difference operators representing linear differential operators. Determining the UNIFAES derivative of the fluctuating component requires computing derivatives of instantaneous velocities at instantaneous conditions and derivatives of mean velocities at mean conditions, as indicated in the right side of eq. (25):

$$\left|\frac{\partial\widetilde{u_\iota}}{\partial x_J}\right| = \left|\frac{\partial(\widetilde{U_\iota+u_\iota})}{\partial x_J}\right|_{U_j+u_j} - \left|\frac{\partial\widetilde{U_\iota}}{\partial x_J}\right|_{U_j} \tag{25}$$

Above procedure differs from applying UNIFAES instantaneous derivation directly to the fluctuating velocity components, as expressed in Eq. (26):

$$\left|\frac{\partial\widetilde{u_\iota}}{\partial x_J}\right|_{U_j+u_j} = \left|\frac{\partial(\widetilde{U_\iota+u_\iota})}{\partial x_J}\right|_{U_j+u_j} - \left|\frac{\partial\widetilde{U_\iota}}{\partial x_J}\right|_{U_j+u_j} \tag{26}$$

In cases with steady mean conditions, linear approximation of UNIFAES differences can be defined by using only the local mean velocity in the cell Peclet number, as follows:

$$\widetilde{\left|\frac{\partial u_\iota}{\partial x_J}\right|}_{U_j} = \left|\frac{\partial(\widetilde{U_\iota+u_\iota})}{\partial x_J}\right|_{U_j} - \widetilde{\left|\frac{\partial U_\iota}{\partial x_J}\right|}_{U_j} \tag{27}$$

3. TRANSPORT EQUATIONS

The transport equation for fluctuating kinetic energy can be written according to the advective – diffusive structure (28), or by expressing the viscous terms with the shear rate, as (29):

$$\frac{\partial U_j\overline{u_i u_i}/2}{\partial x_j} - \nu \frac{\partial^2 \overline{u_i u_i}/2}{\partial x_j \partial x_j} = -\overline{u_i u_j} S_{ij} - \frac{\partial \overline{u_j p}}{\partial x_j} - \frac{\partial \overline{u_j u_i u_i}/2}{\partial x_j} - \nu \overline{\frac{\partial u_i}{\partial x_j}\frac{\partial u_i}{\partial x_j}} \tag{28}$$

$$\frac{\partial U_j\overline{u_i u_i/2}}{\partial x_j} - 2\nu \frac{\partial \overline{u_i s_{ij}}}{\partial x_j} = -\overline{u_i u_j} S_{ij} - \frac{\partial \overline{u_j p}}{\partial x_j} - \frac{\partial \overline{u_j u_i u_i/2}}{\partial x_j} - 2\nu\, \overline{s_{ij} s_{ij}} \tag{29}$$

The transport equation of the “squared vorticity”, or enstrophy, $\overline{w_i w_i/2}$, is (Tennekes and Lumley, 1972):

$$\frac{\partial U_j\overline{w_i w_i/2}}{\partial x_j} - \frac{1}{Re}\frac{\partial^2 \overline{w_i w_i}/2}{\partial x_j \partial x_j} = \overline{w_i s_{ij}} W_j - \overline{w_i u_j}\frac{\partial W_i}{\partial x_j} + \overline{w_i w_j} S_{ij} - \frac{\partial \overline{u_j w_i w_i/2}}{\partial x_j} - \overline{w_i w_j s_{ij}} - \frac{1}{Re}\overline{\frac{\partial w_i}{\partial x_j}\frac{\partial w_i}{\partial x_j}} \tag{30}$$

The transport equation for the velocity-vorticity tensor is deduced by Figueiredo (2018b, eq. 19):

$$\begin{aligned} \frac{\partial \overline{u_i w_k} U_j}{\partial x_j} - \nu \frac{\partial^2 \overline{u_i w_k}}{\partial x_j \partial x_j} = \overline{u_i w_j} S_{kj} - \overline{u_j w_k} S_{ij} + \left(\overline{u_i s_{kj}} - \frac{1}{2}\varepsilon_{ijl}\overline{u_l w_k}\right) W_j - \\ -\overline{u_i u_j}\frac{\partial W_k}{\partial x_j} - \overline{w_k \frac{\partial p}{\partial x_i}} + \overline{u_i w_j s_{kj}} - \frac{\partial \overline{u_i w_k u_j}}{\partial x_j} - 2\nu \overline{\frac{\partial u_i}{\partial x_j}\frac{\partial w_k}{\partial x_j}} \end{aligned} \tag{31}$$

The transport equation for helicity is obtained by contracting indexes i, k into i, i, yielding:

$$\frac{\partial \overline{u_i w_i} U_j}{\partial x_j} - \nu \frac{\partial^2 \overline{u_i w_i}}{\partial x_j \partial x_j} = \frac{\partial \overline{u_i u_j}}{\partial x_j} W_i - \overline{u_i u_j}\frac{\partial W_i}{\partial x_j} - \overline{w_i \frac{\partial p}{\partial x_i}} + \overline{u_i w_j s_{ij}} - \frac{\partial \overline{u_i w_i u_j}}{\partial x_j} - 2\nu \overline{\frac{\partial u_i}{\partial x_j}\frac{\partial w_i}{\partial x_j}} \tag{32}$$

Above expression corrects Eq. (20) of Figueiredo (2018b) with respect to the term proportional to mean vorticity W_i. The error was repeated at Eq. (22) of Figueiredo (2020) and caused slow convergence of the helicity transport equation in the results presented there. Derivation of this term is presented now. After contraction, the factor multiplying the mean vorticity W_j in Eq. (19) results:

$$\overline{u_i s_{ij}} - \frac{1}{2}\varepsilon_{ijl}\overline{u_l w_i} = \overline{u_i s_{ij}} - \frac{1}{2}\varepsilon_{lji}\overline{u_i w_l} = \overline{u_i s_{ij}} + \overline{u_i r_{ji}} = \overline{u_i s_{ij}} - \overline{u_i r_{ij}} = u_i \frac{\partial u_j}{\partial x_i} = \frac{\partial u_i u_j}{\partial x_i} \tag{33}$$

Noticeably, the production terms of helicity equation are related to the mean vorticity and its gradient, while the production term of the kinetic energy equation is related to the mean shear, so that both components of the mean velocity gradient tensor are complementarily considered.

4. RESULTS

Computations refer to the Couette flow sketched at Fig. 1, with normalized dimensions 4x1x1, having lower and upper impermeable adherent walls, with normalized velocity $U_1 = 1$ at $x_2 = 1$, periodic conditions in span-wise direction x_3, Reynolds number 600. Inlet and initial conditions are $\mathcal{U}_i = \mathcal{U}_1(x_2)e_1 = x_2 e_1$, where e_i is versor in direction i. Cubic cells are adopted.

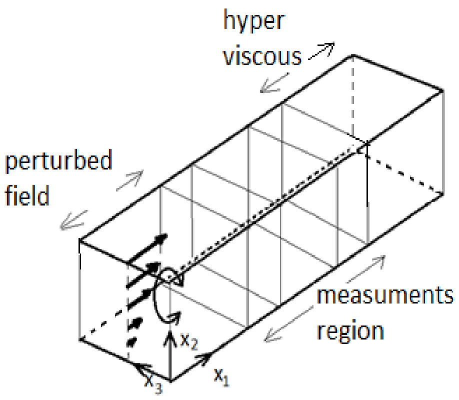

Figure 1 – Domain composed by perturbed field, measurements region and hyper-viscous field.

In the region $0 < x_1 \le 1$, an artificial oscillatory field f induces periodic rotation around x_3 axis:

$$f = M.sin(2\pi\mu t).\beta.\gamma \tag{34}$$

$$\beta = exp\left\{-\left[\frac{\left(x_1 - x_1^O\right)^2}{{\sigma_1}^2} + \frac{\left(x_2 - x_2^O\right)^2}{{\sigma_2}^2} + \frac{\left(x_3 - x_3^O\right)^2}{{\sigma_3}^2}\right]\right\} \tag{35}$$

$$\gamma = [-(x_2 - x_2^O)e_1 + (x_1 - x_1^O)e_2] \tag{36}$$

where $(x_1^O,\ x_2^O,\ x_3^O) = (0.5, 0.5, 0.5),\ M = 2,\ \sigma_1 = \sigma_2 = 0.2,\ \sigma_3 = 0.4$ and $\mu = 0.5$.

In the last part of domain, $3 \leq x_1 < 4$, an hyper viscous fluid reduces the Reynolds number to 10 in order to enforce a steady flow compatible with homogeneous Newman conditions at outlet.

Table 1 presents the values of kinetic energy, helicity and enstrophy in 18 nodes in planes x_1=1.5 and x_1=2.5, for Reynolds number 600 with mesh 240x60x60. The values of helicity and enstrophy depend on the discretization; generally differences are around or below 1%, except at nodes 1 and 3, with differences about 30%. Both forms of UNIFAES present almost coincident results, which are closer to the forth order central differencing than to the second order one.

Table 1. Fluctuations statistics at selected nodes for Re=600 for mesh 240x60x60.

Position		x_1 = 1.5			x_1 = 2.5		
		x_3= 0.25	x_3 = 0.5	x_3= 0.75	x_3= 0.25	x_3 = 0.5	x_3 = 0.75
x_2 = .75	Node	**7**	**8**	**9**	**16**	**17**	**18**
	Kinetic	x10^{-4}	10^{-4}	10^{-4}	10^{-4}	10^{-4}	10^{-4}
	Energy	2.349	3.846	2.349	1.216	1.108	1.216
	Helicity	10^{-3}	10^{-11}	10^{-3}	10^{-3}	10^{-10}	10^{-3}
	CD 2nd	-1.503	3.515	1.503	-1.566	1.057	1.566
	CD 4th	-1.493	3.561	1.493	-1.562	1.060	1.562
	Uni NL	-1.496	3.557	1.496	-1.563	1.060	1.563
	Uni L	-1.496	3.558	1.496	-1.563	1.060	1.563
	Enstrophy	10^{-2}	10^{-2}	10^{-2}	10^{-2}	10^{-3}	10^{-2}
	CD 2nd	1.038	1.024	1.038	1.533	6.280	1.533
	CD 4th	1.047	1.047	1.047	1.534	6.286	1.534
	Uni NL	1.046	1.042	1.046	1.535	6.289	1.535
	Uni L	1.046	1.042	1.046	1.535	6.290	1.535
x_2 = .50	Node	**4**	**5**	**6**	**13**	**14**	**15**
	Kinetic	10^{-3}	10^{-3}	10^{-3}	10^{-4}	10^{-4}	10^{-4}
	Energy	1.127	1.095	1.127	2.756	1.291	2.756
	Helicity	10^{-2}	10^{-10}	10^{-2}	10^{-3}	10^{-10}	10^{-3}
	CD 2nd	-2.659	5.703	2.659	-7.836	5.332	7.836
	CD 4th	-2.671	7.536	2.671	-7.916	5.350	7.916
	Uni NL	-2.669	7.535	2.669	-7.897	5.350	7.897
	Uni L	-2.669	7.536	2.669	-7.898	5.351	7.898
	Enstrophy	10^{-1}	10^{-1}	10^{-1}	10^{-2}	10^{-3}	10^{-2}
	CD 2nd	1.999	1.271	1.999	6.101	3.776	6.101
	CD 4th	2.022	1.285	2.022	6.240	3.807	6.240
	Uni NL	2.018	1.283	2.018	6.208	3.804	6.208
	Uni L	2.018	1.283	2.018	6.208	3.805	6.208
x_2 = .25	Node	**1**	**2**	**3**	**10**	**11**	**12**
	Kinetic	10^{-4}	10^{-4}	10^{-4}	10^{-6}	10^{-6}	10^{-6}
	Energy	1.016	1.076	1.016	6.278	7.929	6.278
	Helicity	10^{-5}	10^{-11}	10^{-5}	10^{-5}	10^{-11}	10^{-5}
	CD 2nd	-6.858	5.629	6.858	1.565	-2.675	-1.565

	CD 4th	-4.628	5.552	4.628	1.477	-2.708	-1.477
	Uni NL	-5.159	5.576	5.159	1.498	-2.701	-1.498
	Uni L	-5.157	5.576	5.157	1.498	-2.701	-1.498
	Enstrophy	10^{-3}	10^{-3}	10^{-3}	10^{-4}	10^{-5}	10^{-4}
	CD 2nd	6.174	1.360	6.174	2.269	8.395	2.269
	CD 4th	6.269	1.371	6.269	2.339	8.505	2.339
	Uni NL	6.246	1.368	6.246	2.321	8.474	2.321
	Uni L	6.245	1.368	6.245	2.321	8.474	2.321

Following the symmetry of the initial perturbation, equal values of kinetic energy and enstrophy are observed in planes z_3 = 0.25 and z_3 = 0.75, as well as opposite values of helicity, which vanishes at central plane z_3 = 0.5. Fluctuating variables generally decay from nodes at plane x_1= 1.5 to corresponding nodes at plane x_1= 2.5, but at level x_2 = 0.75, helicity and particularly enstrophy increase. At level x_2 = 0.25, helicity changes its sign between the two planes. Next Tables refer to node 4.

Table 2 refers to the kinetic energy equation. Advective and pressure term are expressed in advective forms Aa= $U_j\,\partial\overline{(u_\iota u_\iota/2)}/\partial x_j$, Ta= $\overline{u_j\,\partial(u_\iota u_\iota/2)/\partial x_j}$ and Pa= $\overline{u_j\,\partial p/\partial x_j}$ and in divergence forms Ad= $\partial\big(U_j\,\overline{u_\iota u_\iota/2}\big)/\partial x_j$, Td= $\partial\overline{\big(u_j u_\iota u_\iota/2\big)}/\partial x_j$ and Pd= $\partial\overline{u_j p}/\partial x_j$.

Each form of kinetic energy equation derives from one side of equality Vu=Vs, where Vu $= \upsilon\overline{u_\iota\,\partial^2 u_\iota/\partial x_j\partial x_j}$ and Vs $= 2\upsilon\overline{u_\iota\,\partial s_{\iota j}/\partial x_j}$. The first form is decomposed in identity Vu=Df-Du, where Df $= \upsilon\,\partial^2\,\overline{u_\iota u_\iota/2}\,/\partial x_j\partial x_j$ and Du $= \upsilon\overline{\big(\partial u_\iota/\partial x_j\big)\big(\partial u_\iota/\partial x_j\big)}$; the second form according to Vs=Ts-Ds (Eq. 13), where Ts= $\upsilon\,\partial\overline{u_\iota s_{\iota j}}/\partial x_j$ and Ds= $\upsilon\overline{s_{\iota j}s_{\iota j}}$. The production term is P $= \overline{u_\iota u_j}S_{ij}$.

Differences such as Aa≠Ad, Vu≠Df-Du etc., and the spreading of results among the schemes are put as percentage of the term with greater modulus. The divergence form turbulent transport (Td) according to generalized UNIFAES is computed as the difference between the mean advective terms according to non-linear and linear versions. The residuals of the transport equations are presented in absolute value and as percentage of the term with greater modulus.

Table 2 – Statistics of kinetic energy transport equations for Re=600 at node 4 with different numerical schemes and algebraic forms.

Term (or ≠)	40x40x160				60x60x240			
	CD 2nd ord.	CD 4th ord.	Uni L	Spreading	CD 2nd ord.	CD 4th ord.	Uni L	Spreading
Aa (E-4)	-4.911	-4.910	-4.910	0.0	-4.986	-4.985	-4.986	0.0
Ad (E-4)	-4.914	-4.911	-4.911	0.1	-4.987	-4.986	-4.985	0.0
Aa≠Ad	0.1%	0.0%	0.0%		0.0%	0.0%	0.0%	
Ta (E-5)	1.788	1.837	1.835	5.7	1.891	1.914	1.911	1.7
Td (E-5)	1.724	1.807	1.852	6.9	1.863	1.905	1.907	2.3
Ta≠Td	3.6%	1.3%	0.9%		1.5%	0.5%	0.2%	
Pa (E-4)	-7.132	-7.148	-7.132	0.2	-6.938	-6.945	-6.938	0.1
Pd (E-4)	-6.850	-7.056	-6.981	2.9	-6.816	-6.909	-6.875	1.3
Pa≠Pd	4.0%	1.3%	2.1%		1.8%	0.5%	0.9%	
Df (E-4)	-1.328	-1.336	-1.328	0.9	-1.310	-1.314	-1.310	0.4
Du (E-4)	4.127	4.248	4.228	2.8	4.073	4.126	4.116	1.3
Vu (E-4)	-5.540	-5.588	-5.557	0.9	-5.420	-5.441	-5.430	0.4
Vu≠Df-Du	1.5%	0.1%	0.0%		0.7%	0.0%	0.1%	
Ts (E-4)	-3.692	-3.826	-3.795	3.5	-3.767	-3.828	-3.814	1.6
Ds (E-4)	1.508	1.573	1.561	4.1	1.485	1.513	1.508	1.9
Vs (E-4)	-5.372	-5.573	-5.529	3.6	-5.374	-5.436	-5.416	1.1
Vs≠Ts-Ds	3.2%	3.1%	3.1%		2.3%	1.7%	1.7%	
Vs≠Vu	3.0%	0.3%	0.5%		0.8%	0.1%	0.3%	
Pr (E-4)	6.817	6.837	6.832	0.3	6.629	6.637	6.635	0.1
Resid. Eq. 12 (E-5)	-4.085 5.7%	5.465 7.6%	5.294 7.4%		2.773 4.0%	3.379 4.9%	3.291 4.7%	
Resid. Eq. 13 (E-5)	-1.528 2.1%	3.570 5.0%	3.293 4.6%		1.455 2.1%	2.380 3.4%	2.239 3.2%	

Table 3 refers to the helicity equation. Advection and pressure terms of the equation admit advective and divergence forms: Aa=$U_j\,\partial\overline{u_i w_i}/\partial x_j$, Ad=$\partial\left(U_j\overline{u_i w_i}\right)/\partial x_j$, Ta=$\overline{u_j\,\partial(u_i w_i)/\partial x_j}$, Td= $\partial\overline{u_i w_i u_j}/\partial x_j$, Pa= $\overline{w_j\,\partial p/\partial x_j}$ and Pd= $\overline{\partial\left(p w_j\right)/\partial x_j}$. There are two production terms by interaction with mean velocity fields: P1= $\overline{\partial\left(u_i u_j\right)/\partial x_j}\,W_i$ and P2 = $\overline{u_i u_j}\,\partial W_i/\partial x_j$. The fluctuating production term admits distinct algebraic forms: Pt1= $\overline{u_i w_j s_{ij}}$, Pt2= $\overline{w_j\,\partial(u_i u_i/2)/\partial x_j}$ and Pt3= $\partial\left(\overline{w_j u_i u_i}/2\right)/\partial x_j$. The viscous terms of the helicity equation used equality V=Df-Ds, with V= $\upsilon\left(\overline{u_i\,\partial^2 w_i/\partial x_j\partial x_j} + \overline{w_i\,\partial^2 u_i/\partial x_j\partial x_j}\right)$, Df= $\upsilon\,\partial^2\overline{u_i w_i}/\partial x_j\partial x_j$ and Ds = $\upsilon\overline{\left(\partial u_i/\partial x_j\right)\left(\partial w_i/\partial x_j\right)}$.

Table 3 – Statistics of helicity transport equations for Re=600 at node 4 with different numerical schemes and algebraic forms.

Term (or ≠)	40x40x160				60x60x240			
	CD 2nd ord.	CD 4th ord.	Uni L	Spreading	CD 2nd ord.	CD 4th ord.	Uni L	Spreading
Aa (E-3)	6.999	6.954	6.986	0.6	7.292	7.273	7.286	0.3
Ad (E-3)	7.003	6.955	6.983	0.7	7.293	7.274	7.284	0.3
Aa≠Ad	0.1%	0.0%	0.0%		0.0%	0.0%	0.0%	
Ta (E-4)	-3.001	-3.295	-3.223	10.0	-3.547	-3.699	-3.663	4.1
Td (E-4)	-3.063	-3.317	-3.276	7.7	-3.574	-3.709	-3.664	3.6
Ta≠Td	1.3%	0.5%	0.8%		0.0%	0.1%	0.2%	
Pa (E-2)	1.445	1.470	1.461	1.7	1.429	1.440	1.436	0.8
Pd (E-2)	1.439	1.470	1.462	2.1	1.426	1.440	1.436	1.0
Pa≠Pd	0.4%	0.0%	0.1%		0.2%	0.0%	0.0%	
Df (E-3)	5.817	5.920	5.862	1.7	5.716	5.760	5.734	0.8
Du (E-2)	-1.024	-1.060	-1.050	3.4	-1.013	-1.028	-1.024	1.5
Vu (E-2)	1.615	1.652	1.635	2.2	1.588	1.605	1.597	1.1
Vu≠Df-Du	0.6%	0.0%	0.1%		0.2%	0.1%	0.0%	
P1 (E-3)	4.973	5.095	5.064	2.4	4.944	4.998	4.985	1.0
P2 (E-3)	-1.232	-1.267	-1.258	2.8	-1.228	-1.244	-1.240	1.3
Pt1 (E-5)	-4.744	-5.681	-5.211	19.5	-6.473	-6.937	-6.731	6.7
Pt2 (E-5)	-4.801	-5.701	-5.637	23.1	-6.514	-6.942	-6.885	7.0
Pt3 (E-5)	-4.765	-5.629	-5.535	15.3	-6.490	-6.926	-6.858	6.3
≠Pt123	1.2%	1.3%	7.6%		0.6%	0.2%	2.2%	
Resid. Eq. (E-3)	-1.071 7.4%	-1.493 10.2%	-1.366 9.3%		-0.730 5.1%	-0.915 6.4%	-0.857 6.0%	

Table 4 – Statistics of enstrophy transport equations for Re=600 at node 4 with different numerical schemes and algebraic forms.

Term (or ≠)	40x40x160				60x60x240			
	CD 2nd ord.	CD 4th ord.	Uni L	Spreading	CD 2nd ord.	CD 4th ord.	Uni L	Spreading
Aa (E-2)	-8.528	-8.584	-8.600	0.8	-8.701	-8.728	-8.732	0.4
Ad (E-2)	-8.530	-8.585	-8.598	0.8	-8.702	-8.729	-8.732	0.3
Aa≠Ad	0.0%	0.0%	0.0%		0.0%	0.0%	0.0%	
Ta (E-3)	2.763	3.629	3.368	23.9	3.641	4.075	3.959	10.7
Td (E-3)	3.066	3.743	3.399	18.1	3.774	4.113	3.959	8.2
Ta≠Td	9.9%	3.0%	0.9%		3.5%	0.9%	0.0%	
Df (E-2)	-4.918	-5.133	-5.027	4.2	-4.855	-4.948	-4.901	1.9
Du (E-2)	8.571	9.332	9.183	8.2	8.648	8.987	8.917	3.8
Vu (E-2)	-13.791	-14.484	-14.234	4.8	-13.637	-13.938	-13.833	2.2
Vu≠Df-Du	2.2%	0.1%	0.2%		1.0%	0.0%	0.1%	
P1 (E-2)	1.693	1.780	1.757	4.9	1.692	1.731	1.721	2.3
P2 (E-2)	8.002	8.175	8.149	2.1	7.912	7.987	7.974	0.9
P3 (E-2)	-1.345	-1.401	-1.383	4.0	-1.347	-1.372	-1.364	1.8
PT (E-4)	-8.787	-8.320	-8.757	7.9	-6.874	-6.607	-6.794	3.9

Resid. Eq. (E-3)	1.861 2.2%	11.619 12.5%	8.521 9.3%		2.255 2.6%	6.603 7.3%	5.250 5.9%	

Table 4 refers to the enstrophy equation. Mean and turbulent transport terms admit advective and divergent forms: Aa = $\partial\left(U_j \overline{w_\iota w_\iota/2}\right)/\partial x_j$, Ad=$U_j\, \partial\, \overline{w_\iota w_\iota/2}/\partial x_j$, Ta=$\overline{u_j\, \partial(w_\iota w_\iota/2)/\partial x_j}$ and Td = $\partial \overline{u_j\, w_\iota w_\iota/2}/\partial x_j$. The viscous terms results from identity V=Df-Ds, where V= $\upsilon w_i\, \partial^2 w_i/\partial x_j \partial x_j$, Df $= \upsilon\, \partial^2(\overline{w_\iota w_\iota}/2)/\partial x_j \partial x_j$ and Ds= $\overline{\upsilon\left(\partial w_\iota/\partial x_j\right)\left(\partial w_\iota/\partial x_j\right)}$. There are three production terms due to interaction of mean and fluctuating field, P1= $\overline{w_\iota u_j}\, \partial W_i/\partial x_j$, P2= $\overline{w_\iota w_j} S_{ij}$ and P3= $\overline{w_\iota s_{\iota j}} W_j$, and one production term due to the fluctuating field only, Pt = $\overline{w_\iota w_j s_{\iota j}}$.

5. CONCLUSION

For all scalars, differences between advective and divergence forms of the advective term are negligible, as well as differences between the advective terms of the various schemes.

The differences between algebraic forms and the spreading of results between the measuring schemes reduce at ratio generally close to 9:4 from mesh 160x40x40 to mesh 240x60x60, as expected for quadratic behavior. The residuals of the transport equations appear to reduce in sub-quadratic fashion. Second order central differencing usually presented the greater discrepancies between algebraic forms, forth order central differencing the smallest, and UNIFAES intermediate, tending to be closer to the fourth order scheme. However, the second order central differencing was the scheme that presented the smallest unbalances, whilst the fourth order scheme presented the greatest.

This paradox derives from the fact that the various schemes are operating upon the field produced by the solver, which evolves with refinement. Differences between algebraic forms depend solely on the scheme, and in this matter the fourth order scheme shows its expected superiority. But any comparison involving varying refinement depends also on the solver.

Since the generalized UNIFAES scheme employs the interpolating curve of the solver, it may be considered as reference for the solver convergence errors. In this interpretation, the errors of second order central differencing upon the velocity field partially compensates the errors of solver itself, whilst the errors of forth order scheme added to the solver error, in node 4.

6. REFERENCES

Allen, D.N.G., Southwell, R.V., 1955. “Relaxation Methods Applied to Determine the Motion, in Two Dimensions, of a Viscous Flow Pasta Fixed Cylinder”. *Quarterly J. Mechanics and Applied Mathematics*, v.8, 129-145.

Dallas, V. and Tobias, S. M., “Forcing-dependent dynamics and emergence of helicity in rotating turbulence”, J. Fluid Mech., vol.798, pp.682-695, 2016.

Figueiredo, J.R. 2016 “A dynamic statistical equation based model for the turbulent transport of kinetic energy in shear layers”. *Proceedings of Spring School in Transition and Turbulence, EPTT 2016* S. José dos Campos, SP, Brazil.

Figueiredo, J.R. 2018a “Towards a kinetic energy – helicity turbulence model”. *Proceedings of Spring School in Transition and Turbulence EPTT 2018*, Uberlândia, MG, Brasil.

Figueiredo, J.R. 2018b “A statistical dynamic model for the turbulent transport of kinetic energy in shear layers”. *J. Aerosp. Technol. Manag.* 10:e2518, doi:10.5028/jatm.v10.915

Holm, D. D., “Helicity in the formation of turbulence”, Physics of Fluids, vol.19, 2007, 025101.

Llagostera, J. e Figueiredo, J. R., 2000a. “Numerical study on mixed convection in a horizontal flow past a square cavity using UNIFAES scheme” *J. Braz. Society Mech. Sciences*, v.22, 4, 583-597.

Llagostera, J. e Figueiredo, J. R., 2000b. “Application of the UNIFAES discretization scheme to mixed convection in a porous layer with a cavity, using the Darcy model”. *J. Porous Media*, v.3, 2, 16

Moffatt, H. K. and Tsinober, A., “Helicity in laminar and turbulent flow”. Annu. Rev. Fluid Mech. vol.24, pp.281-312, 1992.

Tennekes, H.; Lumley, J.L., 1972, *A First Course in Turbulence*, MIT Press, Cambridge, Massachusetts

Yan, Z., Li, X. and Yu, C. “Scale locality of helicity cascade in physical space”, Phys. Fluids, vol.32, 061705, 2020. doi: 10.1063/5.0013009

7. RESPONSIBILITY NOTICE

The author is the only responsible for the printed material included in this paper.